Fluorescence Enhancement of Coumarin Thiourea Derivatives by Hg^{2+}, Ag^{+}, and Silver Nanoparticles

Ahmed S. Al-Kady,[†] M. Gaber,[†] Mohamed M. Hussein,[‡] and El-Zeiny M. Ebeid*[,†,§]

Chemistry Department, Faculty of Science, Tanta University, Tanta, Egypt, Faculty of Pharmacy, Cairo University, Cairo, Egypt, and Misr University for Science and Technology (MUST), 6th October City, Egypt

Received: June 14, 2009; Revised Manuscript Received: July 1, 2009

Fluorescence enhancement by factors of 5−12 times 8-alkyl thiourido-7-ethoxy-4-methyl coumarin derivatives was observed upon complexation with Hg^{2+}, Ag^{+}, and Ag nanoparticles. The study reveals a chelation-enhanced fluorescence (CHEF) mechanism with the formation of 1:2 complexes in Hg^{2+}/coumarin derivatives and 1:1 complexes in Ag^{+}/coumarin derivatives. The activation parameters of the complexation processes were evaluated with energy of activation values in the case of Ag^{+} being nearly twice those in the case of Hg^{2+}complexation. Isokinetic studies indicate an enthalpy-controlled mechanism in the Hg^{2+}/coumarin derivatives complex formation. No fluorescence enhancement was observed with Fe^{3+}, Co^{2+}, Ni^{2+}, Cu^{2+}, Zn^{2+}, Cd^{2+}, La^{3+}, and Ce^{3+}, making the present coumarin thiourea derivatives selective chemosensors of both $Hg^{2+}$and Ag^{+} ions with different complexation time scales between these two ions. Fluorescence enhancement of the studied coumarin thiourea derivatives using silver nanomaterials occurs almost instantaneously and can be induced by silver nanoparticles in the picomolar (pM) concentration ranges.

Introduction

There is a growing interest to sense heavy metal ions selectively for both chemical and biological reasons. Many analytical methods have been applied in that respect, and much attention has been made to fluorometry because of its low cost, selectivity, sensitivity, and response time.[1,2]

Hg^{2+}, in particular, is a higher toxic environmental pollutant. It exists in the inorganic form or, more seriously, in the organic form as methylmercury, which is even more toxic to aquatic life.[3]

Coumarins are sparsely used as chemical sensors for metal ions based on chelation-enhanced fluorescence (CHEF).[4] In the present derivatives, coumarin moiety is linked to thiourea derivatives with subsequent reduction in fluorescence efficiencies. Upon selective complexation with Hg^{2+}, fluorescence enhancement by a factor of five- to seven-fold takes place.

Several techniques for the determination of mercury ions have been reported over the past few years. These include atomic absorption spectrometry,[5,6] inductively coupled plasma mass spectroscopy,[7−11] spectrophotometry,[12] neutron activation analysis,[13] anodic stripping voltammetry,[14] X-ray fluorescence spectrometry,[15] electrothermal atomic absorption spectrometry,[16] atomic fluorescence spectrometry,[17] and cold vapor atomic absorption spectrometry,[18] and potentiometric ion-selective electrodes for Hg^{2+} ion have been reported.[19−21]

Although these methods have good sensitivity and fast measurement capabilities, they require expensive instruments, well-controlled experimental conditions, and complicated sample-pretreatment procedures. In the past few decades, research interest has focused on developing fluorescent chemosensors for Hg^{2+} because of their sensitive, selectivity, low cost, easy signal detection, and transduction techniques.

TABLE 1: Melting Points and Reaction Yields of Derivatives I−IV

derivative	mp (°C)	% yield
I	208	78
II	208	81
III	130	65
IV	197	58

Some Hg^{2+} sensors are reported that are based on changes in electronic absorption spectra with subsequent color change upon complexation.[22,23] Other Hg^{2+} sensors based on fluorescence enhancement or fluorescence quenching are also reported.[24,25] These are based on moieties of azoderivaties,[22,26] *N*-dansylcarboxamide,[27] chiral polymers,[24] aminonaphthol,[25] anthryl actamide,[28] crown ethers,[29] thiocarbamate,[30] rhodamine,[31−34] naphthalimide,[35] anthraquinone,[36] cholic acid,[30] porphyrin,[37] thiosemicarbazone,[38] carbamodi-thioat,[39] benzothiazole,[40,41] fluorescein,[42,43] phenylenediamine triamide,[44] hydroxyquinoline,[45,46] anthracene,[47,48] and phenoxazinone.[49] Other Hg^{2+} sensors that are based on more complex molecular architecture are reported.[35,50−63]

A gold-nanoparticles (Au NPs)−Rhodamine 6G (Rh6G)-based fluorescent sensor for detecting Hg^{2+} in aqueous solution has been developed. Water-soluble and monodisperse gold nanoparticles (Au NPs) have been prepared facilely and further modified with thioglycolic acid (TGA).[64] Free Rh6G dye was strongly fluorescent in bulk solution. The sensor system composed of Rh6G and Au NPs fluoresces weakly as result of fluorescence resonance energy transfer (FRET) and collision. The fluorescence of the Rh6G- and Au-NPs-based sensor was gradually recovered because the Rh6G units departed from the surface of functionalized Au NPs in the presence of Hg^{2+}.

A chemically programmed antibody sensor, consisting of a stilbenyl boronic acid cofactor and monoclonal antibody EP2-19G2, provides a new method of mercury detection.[65] The fluorescent antibody sensor generates an intense powder blue fluorescence when bound to the stilbenyl boronic acid cofactor;

* Corresponding author. E-mail: drzeiny@yahoo.com.
[†] Tanta University.
[‡] Cairo University.
[§] Misr University for Science and Technology (MUST).

10.1021/jp905566z CCC: $40.75
Published on Web 07/31/2009

TABLE 2: Energy of Activation for Hg^{2+}−Coumarin Complexes

sample	E_a (kJ/mol)	correlation coefficient (r)	standard deviation (SD)
I	56.64	0.99850	0.03621
II	58.01	0.99873	0.03535
III	59.87	0.99917	0.02898
IV	57.28	0.99979	0.01408

TABLE 3: Energy of Activation for Ag^{+}−Coumarin Complexes

sample	E_a (kJ/mol)	correlation coefficient (r)	standard deviation (SD)
I	102.42	0.99925	0.04776
II	109.42	0.99928	0.05031
III	110.38	0.99891	0.06159
IV	107.55	0.99979	0.02611

TABLE 4: (a) First-Order Rate Constants k (s^{-1}) for Hg^{2+}−Coumarin Complexes at Different Temperatures and (b) Activation Parameters for Hg^{2+}−Coumarin Complexes

(a)

sample	k ($\times 10^{-3}$) s^{-1}				
	temperature				
	20 °C	25 °C	30 °C	35 °C	40 °C
I	2.89	4.08	6.07	8.36	12.84
II	2.85	3.97	6.11	8.70	13.13
III	2.72	4.13	5.82	8.69	13.13
IV	2.83	4.11	6.13	8.70	12.77

(b)

sample	ΔE_a (kJ/mol)	$\Delta H^{\#}$ (kJ/mol)	$\Delta G^{\#}$ (kJ/mol)	$\Delta S^{\#}$ (J/mol K)
I	56.64	54.13	86.80	−107.80
II	58.01	55.50	86.79	−103.20
III	59.87	57.36	86.82	−97.20
IV	57.28	54.77	86.79	−105.70

however, it is quenched in the presence of Hg^{2+} ions. The EP2-19G2-cofactor biosensor provides micromolar sensitivity and selectivity toward Hg^{2+} ions over a wide range of metal ions in aqueous solution.

A new series of benzoylthiourea derivatives was prepared, and their chemodosimetric behaviors toward metal cations were investigated in aqueous media at room temperature.[66] Among the various metal cations tested, exclusively the Hg^{2+} ion responds to irreversible color changes of receptors, along with distinctive blue shifts in UV/vis spectra. The receptors can be applicable to the monitoring of Hg^{2+} ion in aqueous solution with a pH span of 4−9.

Several fluorescent sensors for Ag^{+} are reported. A crown-ether-linked iridium(III) complex[67] exhibits a notable luminescence enhancement in the presence of Ag^{+} in aqueous media. A 10-times-higher luminescence enhancement was achieved. A unique chemosensor for Ag^{+} ions was created by coupling an anthracene signaling unit to an amine-terminated glass slide.[68]

A novel dimeric boradiazaindacene dye, which can be converted in one step to an efficient resonance energy transfer (RET) dyad,[69] was applied as a highly selective, emission ratiometric chemosensor for Ag^{+}.

A bicyclic cycloadduct bearing a pyrenyl moiety has been synthesized and investigated as a ratiometric fluorescent sensor for Ag^{1+}.[71] In an aqueous ethanol solution, the presence of silver ion induces the formation of a 1:2 metal−ligand complex, which exhibits a strong intensity enhancement of the pyrene excimer emission at the expense of the emission of monomeric pyrene.

TABLE 5: (a) First-Order Rate Constants for Ag^{+}−Coumarin Complexes at Different Temperatures and (b) Activation Parameters for Ag^{+}−Coumarin Complexes

(a)

sample	k ($\times 10^{-4}$) s^{-1}				
	temperature				
	20 °C	25 °C	30 °C	35 °C	40 °C
I	3.13	6.43	12.83	26.12	53.10
II	3.18	6.42	12.73	28.25	56.68
III	3.08	6.35	12.23	25.83	56.30
IV	3.13	6.43	12.83	26.12	53.10

(b)

sample	ΔE (kJ/mol)	$\Delta H^{\#}$ (kJ/mol)	$\Delta G^{\#}$ (kJ/mol)	$\Delta S^{\#}$ (J/mol K)
I	102.42	99.91	90.67	35.00
II	109.42	106.91	90.55	54.00
III	110.38	107.87	90.64	56.90
IV	107.55	105.04	90.62	47.60

New fluorescent chemosensors, 1,8-bis(pyrazolylmethyl) anthracene and 9,10-bis(pyrazolylmethyl)anthracene, were synthesized.[72] The 1,8-isomer showed selective fluorescence quenching effects with Ag^{+} and Cu^{2+}. However, the 9,10-isomer displayed a selective fluorescence quenching effect only with Ag^{+}.

Coumarins are a group of strongly fluorescent dyes that are sparsely used as efficient chemosensors for transition-metal ions.

A new coumarin based fluorophore having a piperazine moiety as the photoinduced electron transfer (PET) switch was prepared, and its photophysical properties were studied in various solvents and under different PH values.[72] The solvatochromic shift in the fluorescence spectrum revealed an increase in the dipole moment in the lowest excited singlet state compared with that in the ground state. The compound also showed an interesting intramolecular photoinduced proton transfer phenomenon in the excited state under neutral pH. It was effectively utilized as a new CHEF-based chemosensor for zinc and nickel ions in water.

A coumarin azine derivative, 3,3′-hydrazine-1,2-diylidenebis-(methan-1-yl-1-ylidene)bis(7-(diethyl amino)-2*H*-chromen-2-one) (ligand 1), was synthesized and characterized.[73] It was used as a colorimetric chemosensor for Hg^{2+}. The absorption maximum of ligand 1 shows a large red shift from 490 to 565 nm ($\Delta = 75$ nm) in the presence of Hg^{2+}. The change in color is very easily observed by the naked eye, whereas other metal cations, such as Fe^{2+}, Co^{2+}, Ni^{2+}, Zn^{2+}, Cd^{2+}, Cu^{2+}, Fe^{3+}, Ag^{+}, Pb^{2+}, alkali metal, and alkaline earth metal cations, do not induce such a change.

Coumarin derivatives possess a wide range of applications as anticoagulant,[74] antitumor,[75] photosensitizer,[76] anti-HIV,[77] antimicrobial,[78] and antiflammatory agents.[79] Coumarin derivatives have been linked to other molecules in gene expression studies[80] as well as in salmonella detection.[81] Coumarin derivatives are also currently used as fluorogenic dyes in proteomics.[82]

Fluorescence enhancement is gaining increased analytical importance. It allows the use of small quantities of reagents. It also minimizes the background signal and increases selectivity.[83] Different mechanisms of fluorescence enhancement have been proposed. One possible mechanism relies on the lone pair electrons, which normally participated in the fluorescence self-quenching of certain fluorophores. The transfer of these electrons

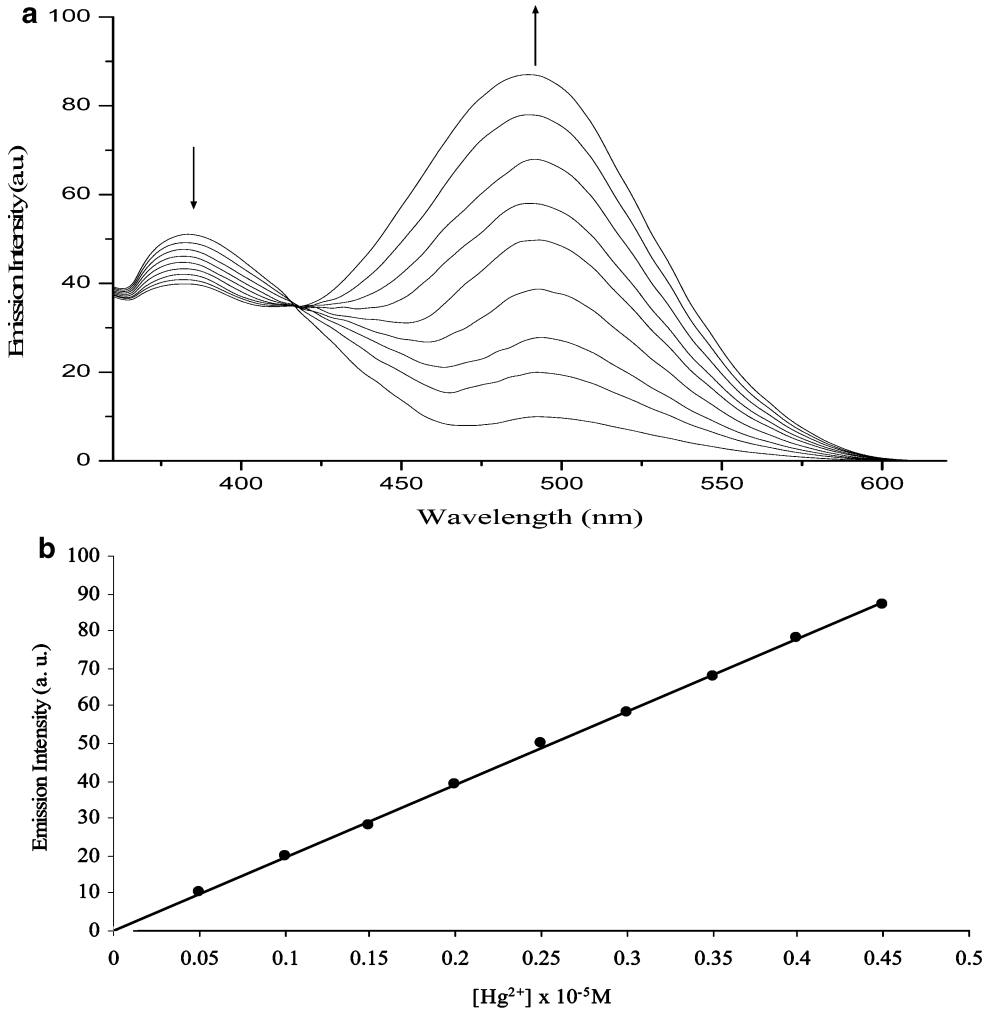

Figure 1. (a) Fluorescence emission spectra of coumarin (10^{-5} M) in the presence of different concentrations of Hg^{2+} at increasing intensities of (0.05, 0.10, 0.15, 0.20, 0.25, 0.30, 0.35, 0.40, and 0.45) $\times$ 10^{-5} M at λ_{ex} = 333 nm and λ_{em} = 488 nm. Emission intensities were measured after 30 min of mixing. (b) Calibration curve using constant concentration of $I = 1.0 \times 10^{-5}$ M in the presence of different concentrations of Hg^{2+} = (0.05 to 0.45) $\times$ 10^{-5} M at λ_{ex} = 333 nm and λ_{em} = 488 nm. Emission intensities were measured after 30 min of mixing.

to the surface plasmon field results in artificial fluorescence enhancement.[84] In addition to the electromagnetic (EM) enhancement, there is a chemical enhancement because of molecule−metal electronic transitions modifying the molecular level structure and transition moments.[85]

In the present article, we report a series of coumarin thiourea derivatives that undergo selective fluorescence enhancement upon complexation with $Hg^{2+}$and Ag^{+} ions. The present series of chemosensors can be easily prepared, and this is advantageous because complicated or time-consuming synthesis may limit chemosensors applications.

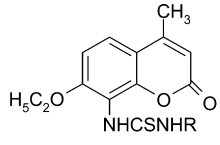

Derivative	R
I	C_2H_5
II	C_3H_5
III	C_6H_5
IV	C_6H_{11}

The fluorescence of compounds I−IV is also remarkably enhanced by silver nanoparticles. Enhanced fluorescence criteria of these coumarin derivatives would be of significant importance in many biological, medical, and chemical fields.

Experimental Section

Steady-state emission spectra were measured using a Shimadzu RF 510 spectrofluorophotometer. The fluorescence spectra were not corrected for machine response. The UV−visible absorption spectra were measured using a Shimadzu UV-160A spectrophotometer connected to a Haake Ultrathermostat.

Mercuric acetate $(CH_3COO)_2Hg$ (99.999%) and silver nitrate ($AgNO_3$) (99.999%) were purchased from Aldrich. Trisodium citrate salt ($C_6H_5O_7Na_3 \cdot 2H_2O$, 95%) was purchased from Fluka.

The complexes are formed by mixing 1 mL of 10^{-4} M of Hg^{2+} or Ag^{+} and 1 mL of 10^{-4} M coumarin derivative in methanol and then making up to the mark with methanol in 10 mL volumetric flasks.

Silver nanoparticles were prepared by the citrate reduction of $AgNO_3$.[86] An aqueous solution of $AgNO_3$ (1 mM, 125 mL) was heated until it began to boil, and then 5 mL of a 1% trisodium citrate solution (as nucleating and reducing agent) was added quickly, which resulted in a change in solution color to pale yellow. After the color change, the solution was removed

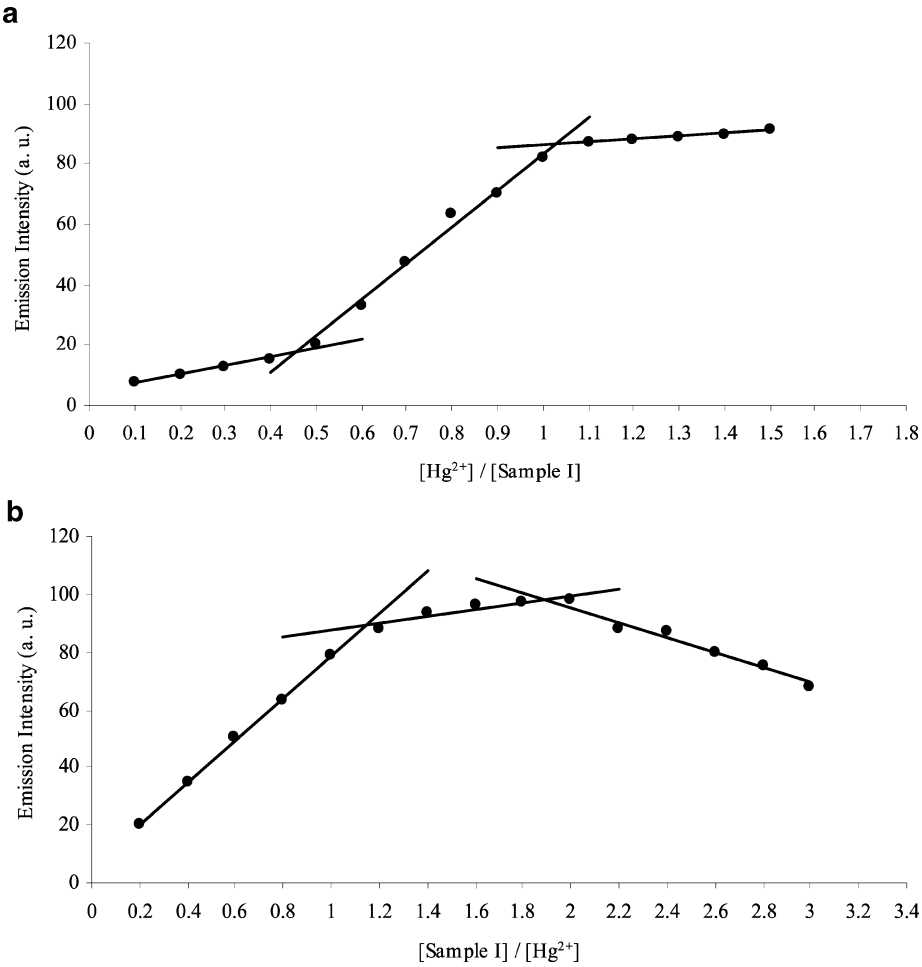

Figure 2. (a) Molar ratio plot of fluorescence intensities of Hg^{2+}/coumarin derivative I complex. The concentration of I was kept constant at 1.0 $\times$ 10^{-5} M in methanol, and we varied the ratio $[Hg^{2+}]/[I]$ by continuously varying $[Hg^{2+}]$ in the range of (0.1 to 1.5) $\times$ 10^{-5} M at λ_{ex} = 333 nm and λ_{em} = 488 nm. Emission intensities were measured after 30 min of mixing. (b) Molar ratio plot of fluorescence intensities of the coumarin derivative I/Hg^{2+} complex. The concentration of Hg^{2+} was kept constant at 1.0 $\times$ 10^{-5} M in methanol, and we varied the ratio $[I]/[Hg^{2+}]$ by continuously varying [I] in the range of (0.1 to 1.5) $\times$ 10^{-5} M at λ_{ex} = 333 nm and λ_{em} = 488 nm.

from the heating element and stirred until it cooled to room temperature. A typical solution of 60−80 nm diameter silver particles that exhibited a characteristic surface plasmon band centered at 420 nm was obtained.

Thiourea derivatives (I−IV) were prepared[87] starting with 4-methyl-7-hydroxy-8-nitrocoumarin. A mixture of 4-methyl-7-hydroxy8-nitrocoumarin (22.1 g; 0.1 mol) was refluxed with anhydrous potassium carbonate (27.6 g; 0.2 mol) and ethyl iodide (23.6 mL; 0.4 mol) in dry acetone (300 mL) with continuous stirring for 15 h and then cooled, filtered, and washed with acetone. The combined filtrate and wash was concentrated and the separated solid was filtered and washed with water and then crystallized from ethanol to give 7-ethoxy-4-methyl-8-nitrocoumarin 179° (90%). A suspension of the nitrocoumarin (10 g) and stannous chloride dihydrate (40 g) in 95% ethyl alcohol (40 mL) and HCl (120 mL) was boiled for 5 min to give a clear solution. The separated crystals obtained after cooling were filtered, suspended in water, and treated with $NaHCO_3$. The yellow solid separated was filtered, extracted with hot isopropanol, and concentrated in vacuum, and the separated shiny yellow crystals were filtered and recrystallized from ethanol to give 8-amino-7-ethoxy-4-methyl−coumarin (7.4 g; mp 127−128° (80%)).

We obtained 8-alkylthiourido 7-ethoxy-4-methyl coumarins (I−IV) by heating a solution of the amine (2.2 g; 0.01 mol in 20 mL of ethanol) with the appropriate isothiocyanate derivative (0.01 mol) in alcohol with stirring for 6 h. The product was concentrated and filtered. The separated solid was recrystallized from ethanol to give the desired compound.

Results and Discussion

The addition of Hg^{2+} to a methanolic solution of coumarin derivative (I) results in the appearance of a new fluorescence band at ca. 488 nm with subsequent quenching of the emission band at ca. 380 nm (Figure 1a). The buildup of the emission band shows a linear relation with the concentration of Hg^{2+} (Figure 1b). No fluorescence enhancement at 488 nm was observed with metal ions Fe^{3+}, Co^{2+}, Ni^{2+}, Cu^{2+}, Zn^{2+}, Cd^{2+}, La^{3+}, and Ce^{3+}.

The molar ratio method studies reveal a two-stage complexation process between Hg^{2+} and coumarin derivatives I−IV. Figure 2a shows the buildup of fluorescence band at 488 nm upon complexation between I (constant concentration) and Hg^{2+} (variable concentrations). Two enhancement criteria are obtained at Hg^{2+}/coumarin molar ratios 1:2 (enhancement factor of about 3) and a molar ratio 1:1 (enhancement factor of about 5). We confirmed this by plotting enhanced fluorescence versus $[I]/[Hg^{2+}]$ molar ratio in which enhancement criteria are obtained at $[I]/[Hg^{2+}]$ molar ratios of 1 and 2 (Figure 2b).

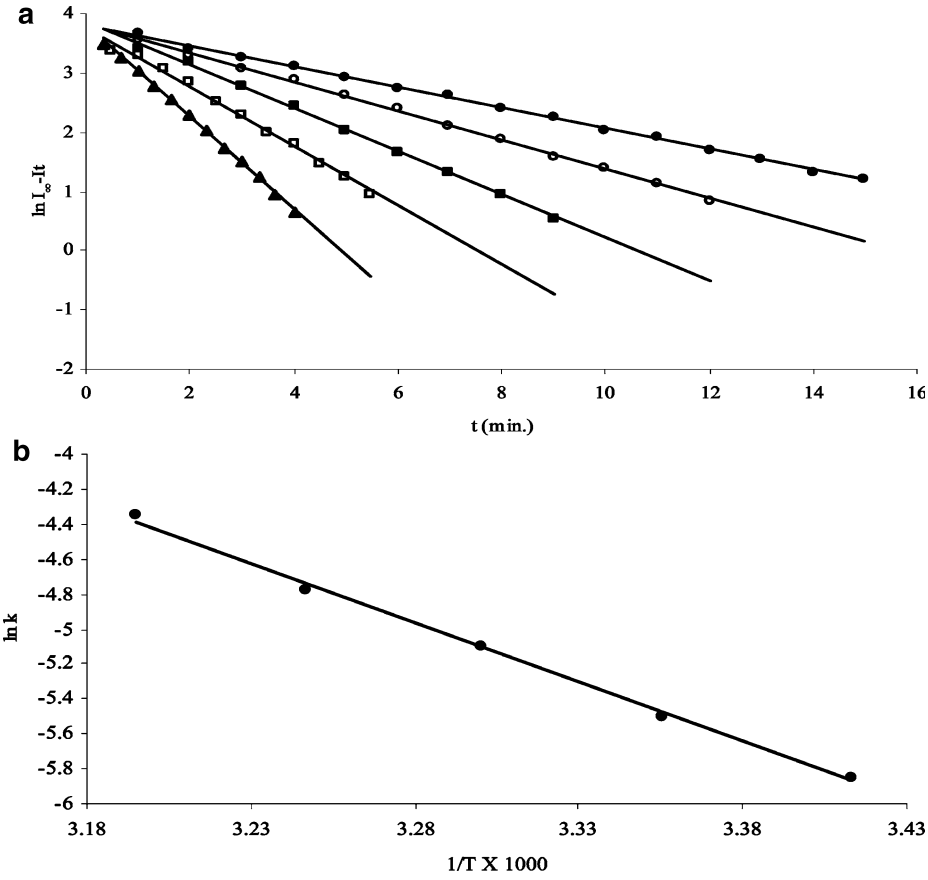

Figure 3. (a) Rate constants of the formation Hg^{2+}−I complex at 20 (●), 25 (○), 30 (■), 35 (□), and 40 °C (▲) upon the addition of $[Hg^{2+}] = 1.0 \times 10^{-5}$ M to $[I] = 1.0 \times 10^{-5}$ M at $\lambda_{ex} = 333$ nm and $\lambda_{em} = 488$ nm. (b) Arrhenius plot for Hg^{2+}−I complex.

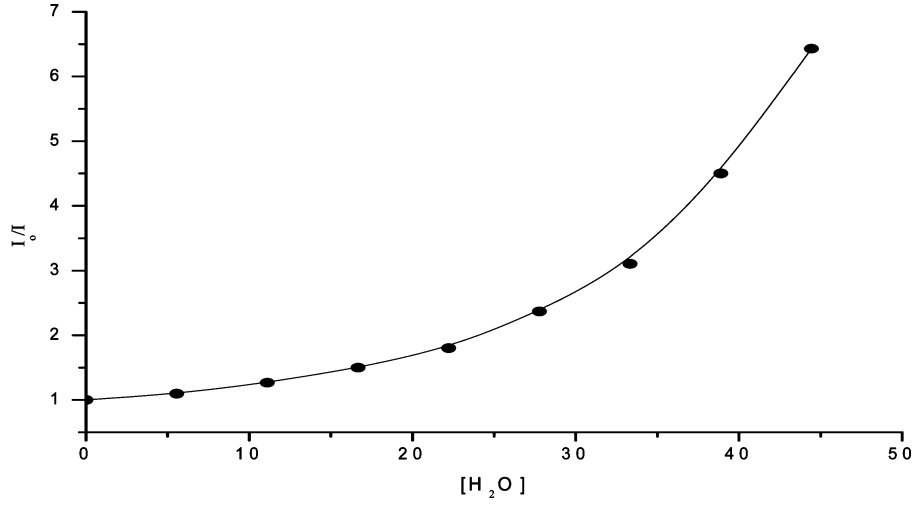

Figure 4. Stern−Volmer plot for the quenching of Hg^{2+}−I complex emission by water. We prepared the complex by mixing 1.0×10^{-5} M of both $[Hg^{2+}]$ and I methanolic solutions. $\lambda_{ex} = 333$ nm and $\lambda_{em} = 488$ nm. Emission intensities were measured after 30 min of mixing.

Similar behaviors are displayed by derivatives II−IV. At 1:1 molar ratio, fluorescence enhancements by factors up to 12 times are achieved.

The fluorescence enhancement is both time- and temperature-dependent, and this is consistent with ground-state complex formation.

Figure 3a shows the first-order kinetic plot of $\ln(I_\infty - I_t)$ versus time for Hg^{2+}−I at different temperatures. From the slopes, the Arrhenius plot was obtained (Figure 3b), from which the energy of activation for the complexation process was obtained as 56.64 kJ mol^{-1}. Derivatives II−IV show similar behavior with Hg^{2+} giving activation energies of 58.01, 59.87, and 57.28 kJ mol^{-1}, respectively (Table 2).

The fluorescence of the Hg^{2+}−coumarin thiourea complex is quenched by water addition. Figure 4 shows the Stern−Volmer plot for quenching of complex Hg^{2+}−I emission by water addition. The plot is not linear and is consistent with a static-type quenching in which water destabilizes the Hg^{2+}−I complex. Similar behavior is displayed by complexes of derivatives II−IV with Hg^{2+}.

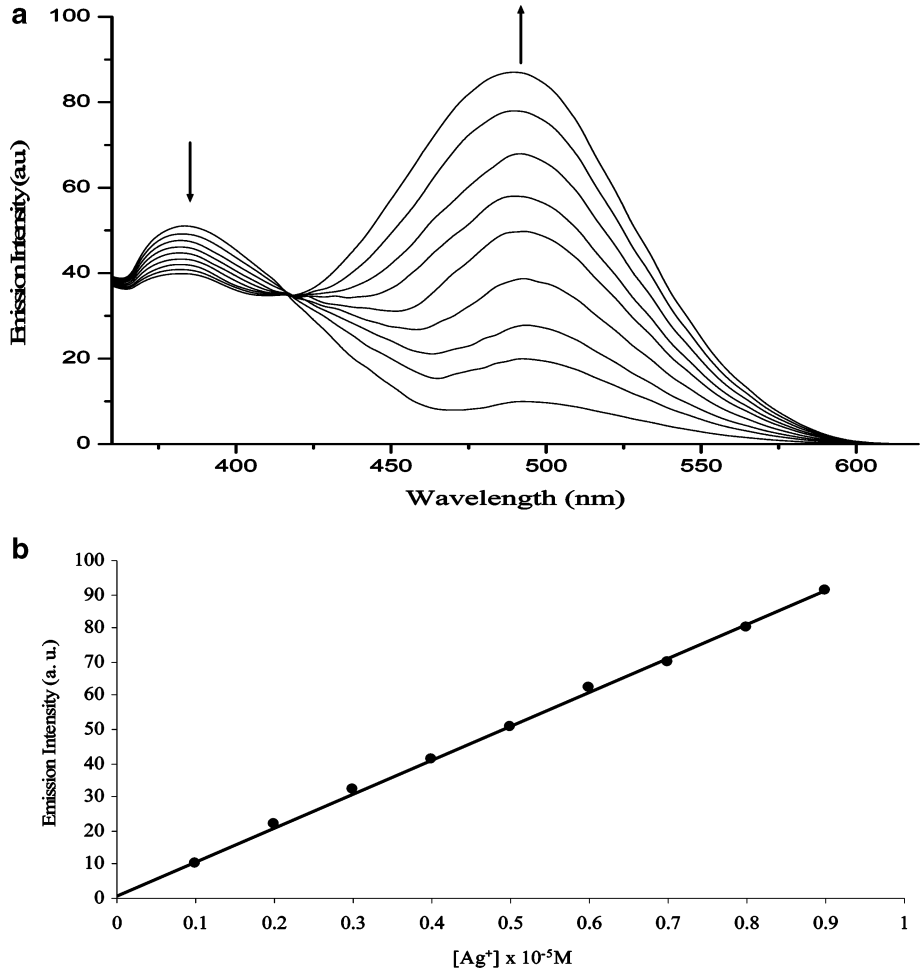

Figure 5. (a) Fluorescence emission spectra of coumarin (10^{-5} M) in the presence of different concentrations of Ag^+ at increasing intensities of (0.05, 0.10, 0.15, 0.20, 0.25, 0.30, 0.35, 0.40, and 0.45) $\times$ 10^{-5} M at $\lambda_{ex} = 333$ nm and $\lambda_{em} = 488$ nm. Emission intensities were measured after 70 min of mixing. (b) Calibration curve using constant concentration of $I = 1.0 \times 10^{-5}$ M in the presence of different concentrations of Ag^+ = (0.05 to 0.45) $\times$ 10^{-5} M at $\lambda_{ex} = 333$ nm and $\lambda_{em} = 488$ nm. Emission intensities were measured after 70 min of mixing.

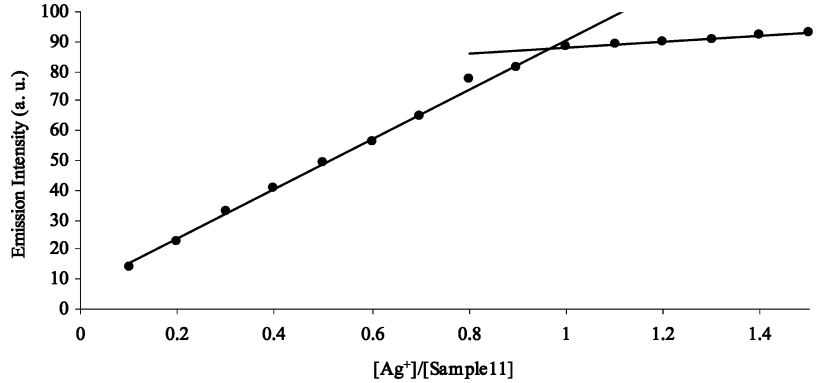

Figure 6. Fluorescence intensity as a function of molar ratio $[Ag^+]$/I at $\lambda_{ex} = 333$ nm and $\lambda_{em} = 488$ nm. The concentration of $I = 1.0 \times 10^{-5}$ M in MeOH and the concentrations of Hg^{2+}were varied from (0.1 to 1.5) $\times$ 10^{-5} M. Emission intensities were measured after 70 min of mixing.

A behavior similar to that of Hg^{2+} complexation was displayed: Ag^+ metal ion with a much larger time scale of complexation process.

The addition of Ag^+ to a methanolic solution of coumarin derivative (I) results in the appearance of a new fluorescence band at ca. 488 nm with subsequent quenching of the emission band at ca. 380 nm (Figure 1a). The buildup of the emission band shows a linear relation with the concentration of Ag^+ (Figure 5b).

Maximum fluorescence enhancement is achieved in 1:1 Ag^+/I molar ratio. This is shown in Figure 6. Similar behaviors are displayed by derivatives II−IV. At 1:1 molar ratio, fluorescence enhancements by factors up to seven times are achieved. This behavior is different from that of Hg^{2+} ions, which binds to two coumarin derivative molecules.

The fluorescence enhancement is both time- and temperature-dependent, and this is consistent with ground-state complex formation.

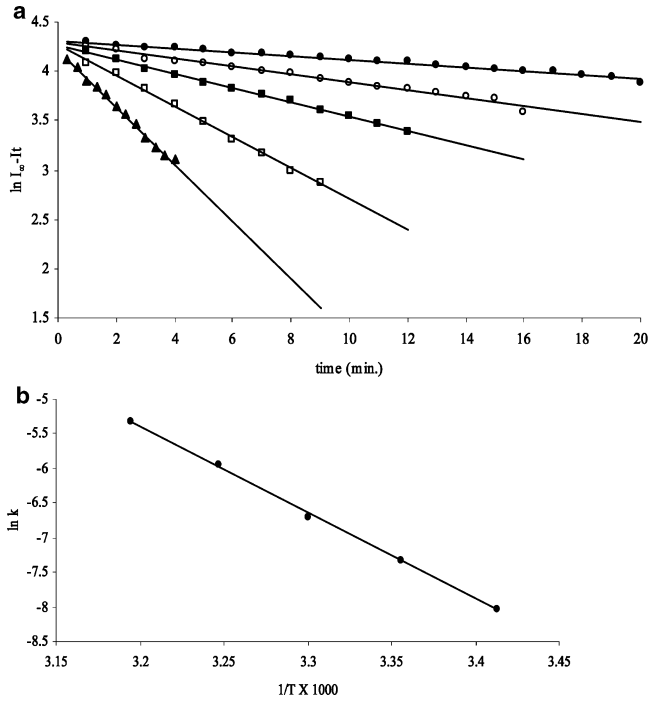

Figure 7. (a) Rate constants of the formation of the $Ag^{+}-I$ complex at 20 (●), 25 (○), 30 (■), 35 (□), and 40 °C (▲) upon the addition of $[Ag^{+}] = 1.0 \times 10^{-5}$ M to $[I] = 1.0 \times 10^{-5}$ M at $\lambda_{ex} = 333$ nm, and $\lambda_{em} = 488$ nm. (b) Arrhenius plot for the $Ag^{+}-I$ complex.

Figure 7a shows the first-order kinetic plot of $\ln(I_\infty - I_t)$ versus time for $Ag^{+}-I$ at different temperatures. From the slopes, the Arrhenius plot was obtained (Figure 7b), from which the energy of activation for the complexation process was obtained as 102.42 kJ mol^{-1}. Derivatives II−IV show behavior similar to that of Hg^{2+}, giving activation energies of 109.42, 110.38, and 107.55 kJ mol^{-1}, respectively (Table 3).

The fluorescence of the $Ag^{+}-I$ complex is quenched by water addition. Figure 8 shows the Stern−Volmer plot for quenching of complex $Ag^{+}-I$ emission by water addition. The plot is not linear and is consistent with a static-type quenching in which water destabilizes the $Ag^{+}-I$ complex. Similar behavior is displayed by complexes of derivatives II−IV with Ag^{+}.

The energies of activation encountered in Ag^{+}-complex formation are nearly twice the values in Hg^{2+}-complex formation (Tables 2 and 3).

The highest activation energy values in both $Hg^{2+}-$coumarin and $Ag^{+}-$coumarin complexes are those with phenyl derivatives. The increased rate of $Hg^{2+}-$coumarin complex formation compared with that of the $Ag^{+}-$coumarin complex is shown in Figure 9. The increased rates displayed by Hg^{2+} compared with Ag^{+} might be of significance in mixture analysis.

The mechanism of fluorescence enhancement upon selective complexation can be explained in terms of the role of lone pair electrons on sulfur and nitrogen atom in the thiourea-linked side chain. These lone pair electrons play a role in fluorescence quenching of parent fluorophore.[87] When this lone pair electrons become encountered in metal ion complexation, fluorescence enhancement occurs. A schematic presentation similar to previously reported systems[84] is given below.

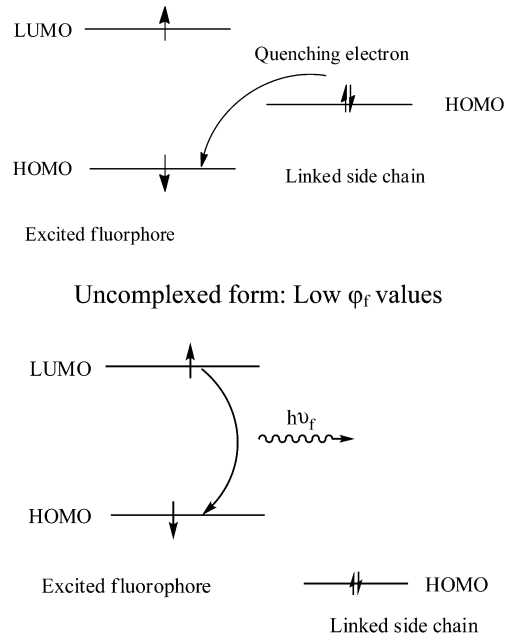

Isokinetic Studies. Table 4a,b gives the rate constants (k, s^{-1}), enthalpies of activation ($\Delta H^{\#}$, kJ/mol), free energies of activation ($\Delta G^{\#}$, kJ/mol), and entropies of activation ($\Delta S^{\#}$, J/mol K) of Hg^{2+} complexes with derivatives I−IV. A plot of $\Delta H^{\#}$

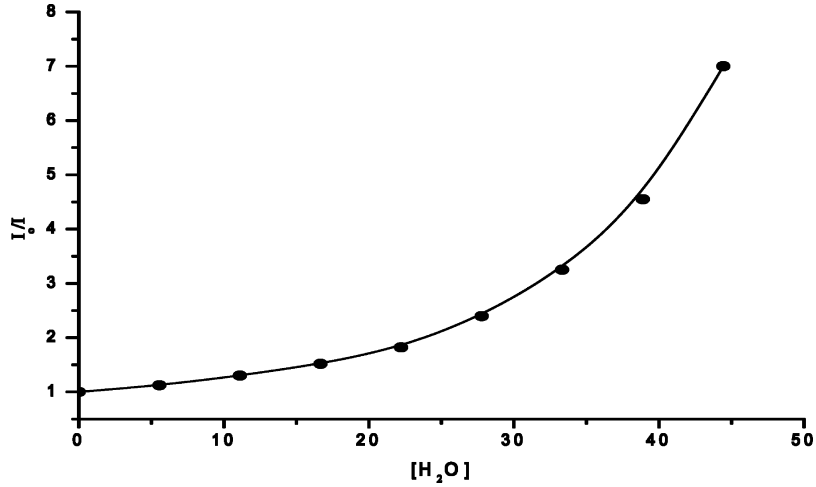

Figure 8. Stern−Volmer plot for the quenching of $Ag^{+}-I$ complex emission by water. We prepared the complex by mixing 1.0×10^{-5} M of both $[Ag^{+}]$ and I methanolic solutions. $\lambda_{ex} = 333$ nm and $\lambda_{em} = 488$ nm. Emission intensities were measured after 70 min of mixing.

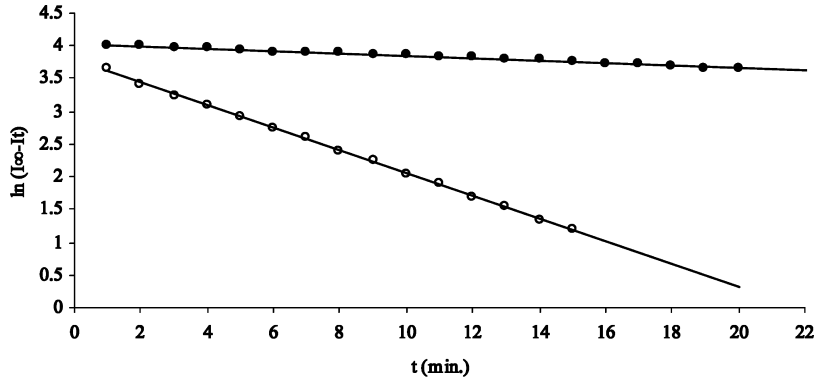

Figure 9. First-order kinetic plots of Ag^{+}−I (●) and Hg^{2+}−I (○) complexes at 20 °C.

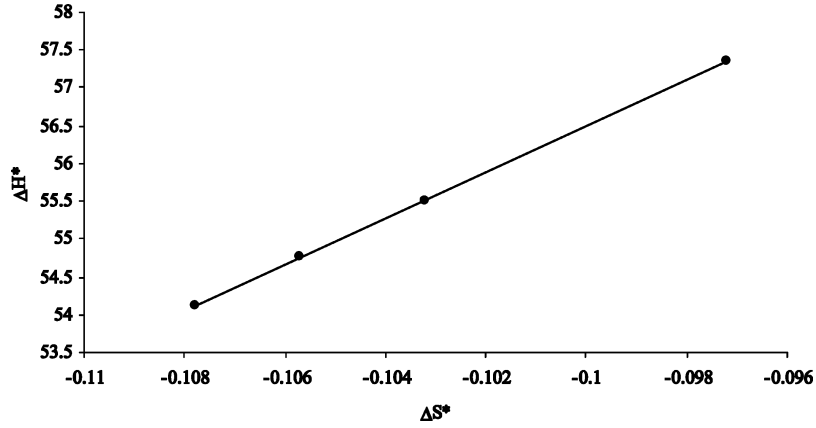

Figure 10. Isokinetic relationship plot of $\Delta H^{\#}$ versus $\Delta S^{\#}$ with a slope of T.

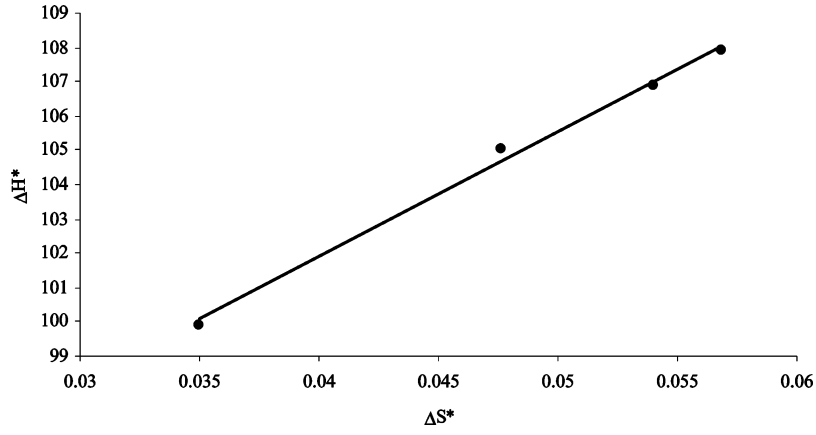

Figure 11. Isokinetic relationship plot of $\Delta H^{\#}$ versus $\Delta S^{\#}$ with a slope of T.

versus $\Delta S^{\#}$ is linear (Figure 10) according to the isokinetic relationship[88]

$$\Delta H^{\#} = T\Delta S^{\#} + C$$

The slope gives the isokinetic temperature $T = 304.58$ K. This temperature is nearly the same as the average experimental temperature of 303 K.

Table 2a,b gives the rate constants (k, s^{-1}), enthalpies of activation ($\Delta H^{\#}$, kJ/mol), free energies of activation ($\Delta G^{\#}$, kJ/mol), and entropies of activation ($\Delta S^{\#}$, J/mol K) of Ag^{+} complexes with derivatives I−IV. A plot of $\Delta H^{\#}$ versus $\Delta S^{\#}$ is linear (Figure 11) with the slope equal to the isokinetic temperature, $T = 363.83$ K. This temperature is higher than the average experimental temperature of 303 K, indicating that the complexation of coumarin derivatives (I−IV) with Ag^{+} ion is an enthalpy-controlled reaction. This is verified by the fact that at the average temperature of 303 K, both enthalpies of activation ($\Delta H^{\#}$, kJ/mol) and rate constants have the same trend.

A remarkable and nearly instantaneous fluorescence enhancement of derivatives I−IV was observed upon the addition of Ag nanoparticles.

About a 14-fold enhancement in fluorescence at 480 nm is achieved within 2 min of mixing Ag nanoparticles and coumarin derivative methanolic solutions. Figure 12 shows the time scale of fluorescence enhancement upon using Ag nanoparticles compared with Ag^{+} ions. In the case of Ag nanoparticles, more enhancement factor is achieved (about 14 fold) compared with

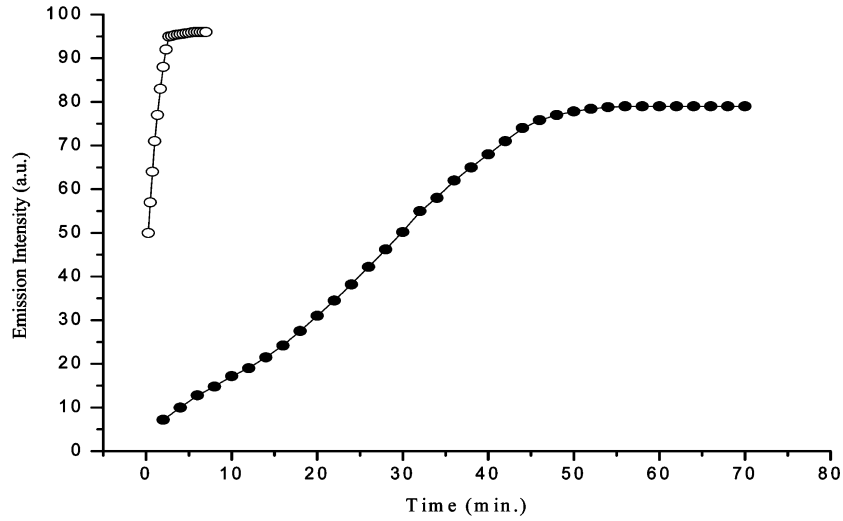

Figure 12. Comparison of time course measurement of fluorescence intensity for Ag nanomaterials (○) and Ag^+ metal ion (●) −I complex.

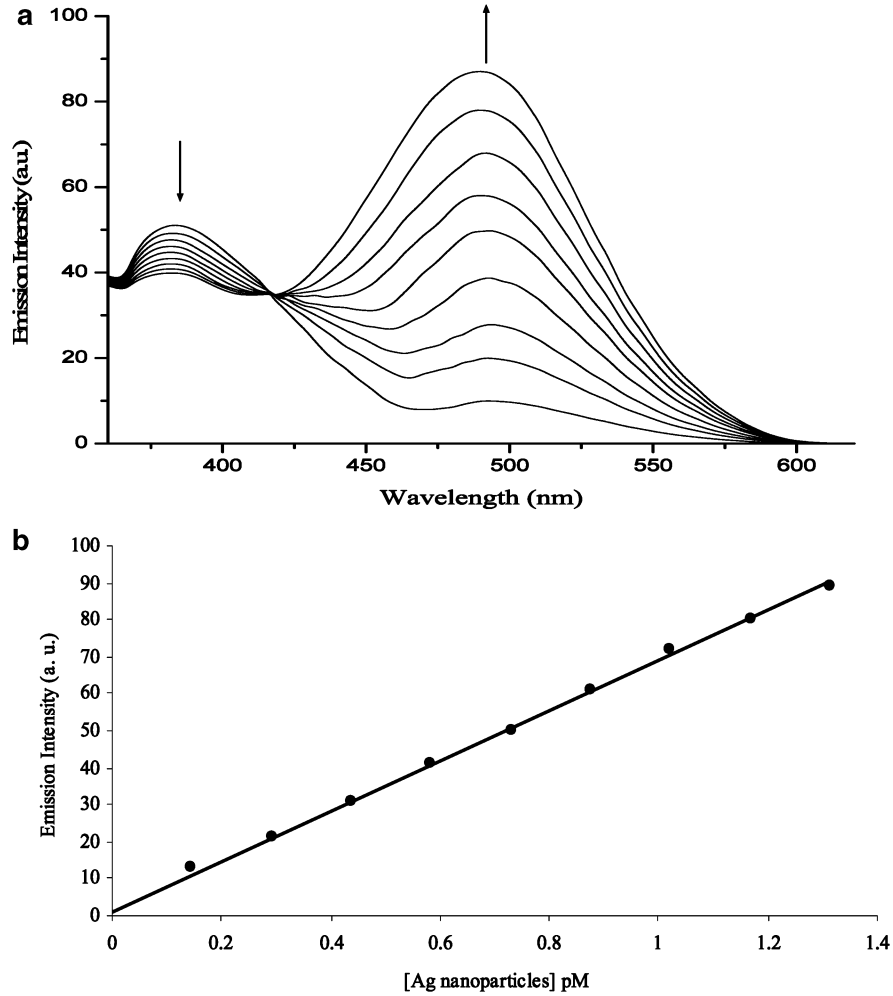

Figure 13. (a) Enhanced fluorescence emission of I (10^{-5} M) as a result of the addition of Ag nanoparticles of concentrations at increasing intensities of 0.146, 0.292, 0.438, 0.584, 0.73, 0.876, 1.022, 1.168, and 1.314 pM at $\lambda_{ex} = 333$ nm and $\lambda_{em} = 489$ nm. Emission intensities were measured after 7 min of mixing. (b) Calibration curve for Ag nanoparticles using constant concentration of $I = 1.0 \times 10^{-5}$ M and different concentrations of Ag nanoparticles in the range of 0.146 to 1.314 pM at $\lambda_{ex} = 333$ nm and $\lambda_{em} = 489$ nm. Emission intensities were measured after 7 min of mixing.

Ag^+ ions. The time scale for full-scale enhancement in the case of Ag nanoparticles is about 20 times shorter than that in Ag^+ ions.

The buildup of the enhanced fluorescence band at 489 nm as a function of Ag nanoparticles addition is shown in Figure 13a. A linear correlation exists between Ag nanoparticles concentration in the picomolar (pM) concentration range and the enhanced fluorescence intensity at 488 nm of I (Figure 13b).

This behavior is of great significance from an analytical point of view because coumarin derivatives can be linked to biological

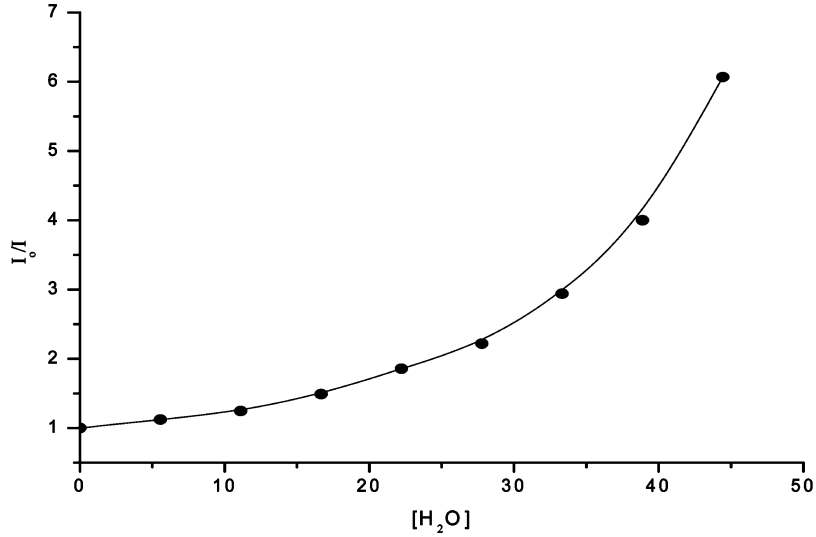

Figure 14. Stern−Volmer plot for the quenching of the Ag nanomaterials−I complex by water. [Ag nanoparticles] = 2.19 pM and [I] = 1.0×10^{-5} M. Maintaining a total volume of 10 mL, the water amount was varied from 1 to 8 mL at λ_{ex} = 333 nm and λ_{em} = 489 nm. Emission intensities were measured after 7 min of mixing.

molecules, followed by selective fluorescence enhancement by the addition of silver nanoparticles.

The addition of water quenches the fluorescence of Ag nanoparticles−coumarin derivatives assemblies. Figure 14 shows the Stern−Volmer plots of fluorescence quenching of derivative (I) assembly with Ag nanomaterial upon using water as a quencher. No significant quenching is achieved below a water percentage of about 20% in methanol. This is also of analytical significance because aqueous media are of importance in many biological systems.

The fluorescence quenching induced by water can be explained according to the role of water as a polar solvent in stabilizing the polar excited state and thus lowers the transition momentum to ground state via radiationless transitions.[89] A second mechanism of water quenching is via hydrogen bonding with nitrogen and sulfur coordination atoms or acting as replacing ligands that undergo coordination with metal ions at the expense of coumarin derivatives I−IV.

References and Notes

(1) Chattopadhyay, N.; Mallick, A.; Sengupha, S. *J. Photochem. Photobiol., A* **2006**, *177*, 55–60.
(2) Young, S. *Spectrochim. Acta A* **2007**, *68*, 705–709.
(3) Harris, H.; Pickering, I. J.; George, G. N. *Science* **2003**, *301*, 1203.
(4) de Silva, A. P.; Gunaratne, H. Q. N.; Gunnlaugsson, T.; Huxley, A. J. M.; McCoy, C. P.; Rademacher, J. T.; Rice, T. E. *Chem. Rev.* **1997**, *97*, 1515–1566.
(5) Kopysc, E.; Pyrzynska, K.; Garbos, S.; Bulska, E. *Anal. Sci.* **2000**, *16*, 1309–1312.
(6) Cizdziel, J. V.; Gerstenberger, S. *Talanta* **2004**, *64*, 918–921.
(7) Karunasagar, D.; Arunachalam, J.; Gangadharan, S. *J. Anal. At. Spectrom.* **1998**, *13*, 679–682.
(8) Harrington, C. F.; Merson, S. A.; D'Silva, T. M. D. *Anal. Chim. Acta* **2004**, *505*, 247–254.
(9) Anthemidis, A. A. N.; Zachariadis, G. A.; Michos, C. E.; Stratis, J. A. *Anal. Bioanal. Chem.* **2004**, *379*, 764–769.
(10) Trimble, C. A.; Hoenstine, R. W.; Highley, A. B.; Donoghue, J. F.; Ragland, P. C. *Mar. Georesour. Geotechnol.* **1999**, *17*, 187–197.
(11) Smigelski, T.; O'Brien, K.; Fusco, J.; Schaumloffel, J. C.; Tausta, J. 226th National Meeting of the American Chemical Society, September 7−11, 2003.
(12) Marczenko, Z. *Separation and Spectrophotometric Determination of Elements*; Ellis Horwood: Chichester, U.K., 1986.
(13) Yu, J. C.; Lo, J. M.; Wai, K. M. *Anal. Chim. Acta* **1983**, *154*, 307–312.
(14) Ugo, P.; Mortto, L.; Bertoneell, P.; Wang, J. *Electroanalysis* **1998**, *10*, 1017–1021.
(15) Bennun, L.; Gomez, J. *Spectrochim. Acta, Part B* **1997**, *52*, 1195–1200.
(16) Burrini, C.; Cagnini, A. *Talanta* **1997**, *44*, 1219–1223.
(17) Safawi, A.; Eddon, L.; Foulkes, M.; Stockwell, P.; Corns, W. *Analyst* **1999**, *124*, 185–189.
(18) Yamini, Y.; Alizadeh, N.; Shamsipur, M. *Anal. Chim. Acta* **1997**, *355*, 69–74.
(19) Buhlmann, P.; Pretsch, E.; Bakker, E. *Chem. Rev.* **1998**, *98*, 1593–1688.
(20) Fakhari, A. R.; Ganjali, M. R.; Shamsipur, M. *Anal. Chem.* **1997**, *69*, 3693–3696.
(21) Pérez-Marín, L.; Otazo-Sánchez, E.; Macedo-Miranda, G.; Avila-Pérez, P.; Chamaro, J. A.; López-Valdivia, H. *Analyst* **2000**, *125*, 1787–1790.
(22) Cheng, Y.; Zhang, M.; Yang, H.; Li, F.; Yi, T.; Huang, C. *Dyes Pigm.* **2008**, *76*, 775–783.
(23) Sheng, R.; Wu, S. *Sens. Actuators, B* **2008**, *128*, 507–511.
(24) Liu, Y.; Zong, L.; Zheng, L.; Wu, L.; Cheng, Y. *Polymer* **2007**, *48*, 6799–6807.
(25) Young, S. *Spectrochim. Acta, Part A* **2007**, *68*, 705–709.
(26) Cheng, Y.; Zhao, D.; Zhang, M.; Liu, Z.; Zhou, Y.; Shu, T.; Li, F.; Yi, T.; Huang, C. *Tetrahedron Lett.* **2006**, *47*, 6413–6416.
(27) Talanov, V. S.; Roper, E. D.; Buie, N. M.; Talanova, G. G. *Tetrahedron Lett.* **2007**, *48*, 8022–8025.
(28) Song, K. C.; Kim, M. H.; Kim, H. J.; Chang, S. K. *Tetrahedron Lett.* **2007**, *48*, 7464–7468.
(29) Meng, X. M.; Zhu, M. Z.; Guo, Q. X. *Chin. Chem. Lett.* **2007**, *18*, 1209–1212.
(30) Wang, H.; Chan, W. *Tetrahedron* **2007**, *63*, 8825–8830.
(31) Zhang, X.; Shiraishi, Y.; Hirai, T. *Tetrahedron Lett.* **2007**, *48*, 5455–5459.
(32) Lee, M. H.; Cho, B.; Yoon, J.; Kim, J. S. *Org. Lett.* **2007**, *9*, 4515–4518.
(33) Yang, Y.; Yook, K.; Tae, J. *J. Am. Chem. Soc.* **2005**, *127*, 16760–16761.
(34) Zheng, H.; Qian, Z.; Xu, L.; Yuan, F.; Lan, L.; Xu, J. *Org. Lett.* **2006**, *8*, 859–861.
(35) Mu, H.; Gong, R.; Ma, Q.; Sun, Y.; Fu, E. *Tetrahedron Lett.* **2007**, *48*, 5525–5529.
(36) Yang, H.; Zhou, Z.; Xu, J.; Li, F.; Yi, T.; Huang, C. *Tetrahedron* **2007**, *63*, 6732–6736.
(37) Dolci, L. S.; Marzocchi, E.; Montalti, M.; Prodi, L.; Monti, D.; Di Natale, C.; D'Amico, A.; Paolesse, R. *Biosens. Bioelectron.* **2006**, *22*, 399–404.
(38) Yu, Y.; Lin, L.; Yang, K.; Zhong, X.; Huang, R.; Zheng, L. *Talanta* **2006**, *69*, 103–106.
(39) Meng, X.; Liu, L.; Hu, H.; Zhu, M.; Wang, M.; Shi, J.; Guo, Q. *Tetrahedron Lett.* **2006**, *47*, 7961–7964.
(40) Song, K. C.; Kim, J. S.; Park, S. M.; Chung, K.; Ahn, S.; Chang, S. *Org. Lett.* **2006**, *8*, 3413–3416.
(41) Tatay, S.; Gavina, P.; Coronado, E.; Palomares, E. *Org. Lett.* **2006**, *8*, 385738–60.

(42) Nolan, E. M.; Racine, M. E.; Lippard, S. J. *Inorg. Chem.* **2006**, *45*, 2742.
(43) Nolan, E. M.; Lippard, S. J. *J. Am. Chem. Soc.* **2003**, *125*, 14270–14271.
(44) Wang, J.; Qian, X. *Chem. Commun.* **2006**, 109.
(45) Zhang, H.; Han, L.; Zachariasse, K. A.; Jiang, Y. *Org. Lett.* **2005**, *7*, 4217–4220.
(46) Moon, S. Y.; Cha, N. R.; Kim, Y. H.; Chang, S. *J. Org. Chem.* **2004**, *69*, 181–183.
(47) Bolletta, F.; Garelli, A.; Montalti, M.; Prodi, L.; Romano, S.; Zaccheroni, N.; Canovese, L.; Chessa, G.; Santo, C.; Visentin, F. *Inorg. Chim. Acta* **2004**, *357*, 4078–4084.
(48) Yoon, J.; Ohler, N. E.; Vance, D. H.; Aumiller, W. D.; Czarnik, A. W. *Tetrahedron Lett.* **1997**, *38*, 3845–3848.
(49) Descalzo, A. B.; Máñez, R. M.; Radeglia, R.; Rurack, K.; Soto, J. *J. Am. Chem. Soc.* **2003**, *125*, 3418–3419.
(50) Yuan, M.; Li, Y.; Li, J.; Li, C.; Liu, X.; Lv, J.; Xu, J.; Liu, H.; Wang, S.; Zhu, D. *Org. Lett.* **2007**, *9*, 2313–2316.
(51) Praveen, L.; Ganga, V. B.; Thirumalai, R.; Sreeja, T.; Reddy, M. L. P.; Varma, R. L. *Inorg. Chem.* **2007**, *46*, 6277–6282.
(52) Othman, A.; Lee, J. W.; Wu, J.; Kim, J. S.; Abidi, R.; Thuéry, P.; Strub, J. M.; Dorsselaer, A.; Vicens, J. *J. Org. Chem.* **2007**, *72*, 7634–7640.
(53) Wu, J.; Hwang, I.; Kim, K. S.; Kim, J. S. *Org. Lett.* **2007**, *9*, 907–910.
(54) Kim, S. H.; Song, K. C.; Ahn, S.; Kang, Y. S.; Chang, S. *Tetrahedron Lett.* **2006**, *47*, 497–500.
(55) Wu, Z.; Zhang, Y.; Ma, J. S.; Yang, G. *Inorg. Chem.* **2006**, *45*, 3140–3142.
(56) Wang, Z.; Zhang, D.; Zhu, D. *Anal. Chim. Acta* **2005**, *549*, 10–13.
(57) Youn, N.; Chang, S. *Tetrahedron Lett.* **2005**, *46*, 125–129.
(58) Chen, Q.; Chen, C. *Tetrahedron Lett.* **2005**, *46*, 165–168.
(59) Kao, T.; Wang, C.; Pan, Y.; Shiao, Y.; Yen, J.; Shu, C.; Lee, G.; Peng, S.; Chung, W. *J. Org. Chem.* **2005**, *70*, 2912–2920.
(60) Coronado, E.; Galán-Mascarós, J. R.; Martí-Gastaldo, C.; Palomares, E.; Durran, J. R.; Vilar, R.; Gratzel, M.; Nazeeruddin, M. K. *J. Am. Chem. Soc.* **2005**, *127*, 12351–12356.
(61) Guo, X.; Qian, X.; Jia, L. *J. Am. Chem. Soc.* **2004**, *126*, 2272–2273.
(62) Zhang, X.; Guo, C.; Li, Z.; Shen, G.; Yu, R. *Anal. Chem.* **2002**, *74*, 821–825.
(63) Talanova, G. G.; Elkarim, N. S. A.; Talanov, V. S.; Bartsch, R. A. *Anal. Chem.* **1999**, *71*, 3106–3109.
(64) Chen, J.; Zheng, A.; Chen, A.; Gao, Y.; He, C.; Kai, X.; Wu, G.; Chen, Y. *Anal. Chim. Acta* **2007**, *599*, 134–142.
(65) Matsushita, M.; Meijler, M. M.; Wirsching, P.; Lerner, R. A.; Janda, K. D. *Org. Lett.* **2005**, *7*, 4943–4946.
(66) Lee, M. H.; Wu, J.; Lee, J. W.; Jung, J. H.; Kim, J. S. *Org. Lett.* **2007**, *9*, 2501–2504.
(67) Schmittel, M.; Lin, H. *Inorg. Chem.* **2007**, *46*, 9139–9145.
(68) Shin, D. H.; Kim, W. N.; Ko, Y. G.; Choi, U. S. *Ind. Eng. Chem. Res.* **2006**, 656–662.
(69) Coskun, A.; Akkaya, E. U. *J. Am. Chem. Soc.* **2005**, *127*, 10464–10465.
(70) Yang, R.; Chan, W.; Lee, A. W. M.; Xia, P.; Zhang, H.; Li, K. *J. Am. Chem. Soc.* **2003**, *125*, 2884–2885.
(71) Kang, J.; Choi, M.; Kwon, J. Y.; Lee, E. Y.; Yoon, J. *J. Org. Chem.* **2002**, *67*, 4384–4386.
(72) Chattopadhyay, N.; Mallick, A.; Sengupta, S. *J. Photochem. Photobiol., A* **2006**, *177*, 55–60.
(73) Sheng, R.; Wang, P.; Liu, W.; Wu, S. *Sens. Actuators, B* **2008**, *128*, 507–511.
(74) Lowenthal, J.; Birnbaum, H. *Science* **1969**, *164*, 181–183.
(75) Nair, R. V.; Fisher, E. P.; Safe, S. H.; Cortez, C.; Harvey, R. G.; DiGiovanni, J. *Carcinogenesis* **1991**, *12*, 65–69.
(76) Bryantseva, G.; Sokolova, I. V.; Tsyrenzhapova, A. B.; Selivanov, N. I.; Khilya, V. P.; Garazd, Ya. L. *J. Appl. Spectrosc.* **2008**, *75*, 700–705.
(77) Spino, C.; Dodier, M.; Sotheeswaran, S. *Bioorg. Med. Chem. Lett.* **1998**, *8*, 3475–3478.
(78) Cottigli, F.; Loy, G.; Garau, D.; Floris, C.; Caus, M.; Pompei, R.; Bonsignore., L. *Phytomedicine* **2001**, *8*, 302–305. Zavrsnik, D.; Muratović, S.; Spirtović, S.; Softić, D.; Medić-Sarić, M. *Bosn. J. Basic Med. Sci.* **2008**, *8*, 277–281. Kawase, M.; Varu, B.; Shah, A.; Motohashi, N.; Tani, S.; Saito, S.; Debnath, S.; Mahapatra, S.; Dastidar, S. G.; Chakrabarty, A. N. *Arzneim. Forsch.* **2001**, *51*, 7–71. El-Fattah, M. E. *Arch. Pharm. Res.* **1998**, *21*, 723–728.
(79) Fylaktakidou, K. C.; Hadjipavlou-Litina, D. J.; Litinas, K. E.; Nicolaides, D. N. *Curr. Pharm. Des.* **2004**, *10*, 3813–3833.
(80) Zlokarnik, G.; Negulescu, P. A.; Knapp, T. E.; Mere, L.; Burres, N.; Feng, L.; Whitney, M.; Roemer, K.; Tsien, R. Y. *Science* **1988**, *279*, 84. Weinzierl, R. O. J. Chapter 9. In *Mechanisms of Gene Expression*; Imperial College Press: London, 1999.
(81) Aguirre, P. M.; Cacho, J. B.; Folgueira, L.; Lopez, M.; Garcia, J.; Velasco, A. C. J. *Clin. Microbiol.* **1990**, *28*, 148–149. Manafi, M.; Kneifel, W.; Bascomb, S. *Microbiol. Rev.* **1991**, *55*, 335–348.
(82) Beatty, K. E.; Liu, J. C.; Xie, F.; Dieterich, D. C.; Schuman, E. M.; Wang, Q.; Tirrell, D. A. *Angew. Chem., Int. Ed.* **2006**, *45*, 7364–7367.
(83) Hong, B.; Tang, L.; Ren, Y.; Kang, K. A. In *Advances of Experimental Medicine and Biology*; Maguire, D. J., Bruley, D. F., Harris, D. K., Eds.; Springer: New York, 2007; p 23.
(84) (a) Lakowicz, J. R. *Principles of Fluorescence Spectroscopy*; Springer: Singapore, 2006; p 642. (b) Kubo, K. In *Topics in Fluorescence Spectroscopy: Advanced Concepts in Fluorescence Sensing: Macromolecular Sensing*; Geddes, C. D., Lakowicz, J. R., Eds.; Plenum Press: New York, 2005; Vol. 9, pp 219−247.
(85) Gray, S. K. *Plasmonics* **2007**, *2*, 143–146.
(86) (a) Guzmán, M. G.; Dille, J.; Godet, S. *Proc. World Acad. Sci., Eng., Technol.* **2008**, *33*, 367–374. (b) Ebeid, E. M.; AlHazmy, S. M. *Photophysical and Laser-Based Techniques in Chemistry, Biology, and Medicine*; BookSurge, LLC: Charleston, SC, 2006; p 169.
(87) (a) Shah, N. M.; Mehta, D. H. *J. Ind. Chem. Soc.* **1954**, *31*, 784–786. (b) Ebeid, M. Y.; Amin, K. M.; Hussein, M. M. *Egypt. J. Pharm. Sci.* **1987**, 183–191.
(88) (a) Farrar, D. H.; Fei, R.; Poe, A. J. *Inorg. Chim. Acta* **2008**, *361*, 3125–3134. (b) House, J. E. *Principles of Chemical Kinetics*; Brown Publishers: Chicago, 1997; p 162.
(89) Suppan, P.; Ghoneim, N. In *Solvatochromism*; The Royal Society of Chemistry: Cambridge, U.K., 1997; p 12.

JP905566Z